

# Measurements of Phase Behavior for Polyethylene in Hydrocarbons, Halogenated Hydrocarbons, and Oxygen-Containing Hydrocarbons, at High Pressure and High Temperature<sup>†</sup>

Junich Kojima,<sup>‡</sup> Mikihiro Takenaka,<sup>\*,§</sup> Yoshiaki Nakayama,<sup>‡</sup> and Susumu Saeki<sup>||</sup>

Asahi Kasei Fibers Corporation, Moriyama Shiga 524-0002, Japan, Department of Polymer Chemistry, Graduate School of Engineering, Kyoto University, Kyoto 615-8510, Japan, and Department of Materials Science and Engineering, Fukui University, Fukui 910-8507, Japan

Phase behaviors of high molecular weight polyethylene solutions with hydrocarbons, halogenated hydrocarbons, and oxygen-containing hydrocarbons and their mixture as solvents were examined under high temperature and high pressure, especially near the critical and supercritical condition of the solvent. The pressure–temperature ( $P,T$ ) cloud point curves for polyethylene in pentane, trichlorofluoromethane, and hexane were measured at different compositions. The pressure–composition ( $P,C$ ) cloud point curves at 473 K are presented for three systems. The  $P,T$  cloud point curves for volume fraction,  $\phi = 2\%$ , of high molecular weight polyethylene were measured in different hydrocarbons and halogenated hydrocarbons. It was found that the cloud point pressures of the solutions have good correlation with the critical temperature ( $T_c$ ) of solvents. The  $P,T$  cloud point curves for  $\phi = 2\%$  of high molecular weight polyethylene were measured in different hydrocarbon and pentane mixtures, different halogenated hydrocarbon and pentane mixtures, and different oxygen-containing hydrocarbon and pentane mixtures at volume ratio 50/50. The  $P,T$  cloud point curves for high molecular weight polyethylene in mixed solvents of 1,1-dichloro-2,2,2-trifluoroethane (HCFC123) + cyclohexane with volume ratio of 75/25 were also measured as a function of polymer composition.

## Introduction

Phase behaviors of polyethylene (PE) in ethylene, ethane, and the higher paraffin at high pressure and high temperature have been investigated for decades. Various kinds of cells were used to determine the cloud point curves of the PE solutions.

Ehrlich and Kurpen<sup>1</sup> investigated the phase behavior of PE with molecular weight from 17 000 to 246 000 in ethane, propane, butane, and pentane. The PE solutions exhibit upper critical solution pressure type phase diagrams. As similar to usual polymer solutions, the critical polymer concentrations of the PE solutions were low and shift to lower concentration with molecular weight.

de Loos et al.<sup>2,3</sup> prepared several well-characterized linear PE and measured the cloud point curves of the linear PE/ethylene solutions at (380 to 445) K and (90 to 200) MPa. Then they compared the cloud point curves obtained from their experiments with those calculated with the extended Flory–Huggins theory by Koningsveld and Kleintjens and found good agreement between them.

Condo et al.<sup>4</sup> then measured the phase behavior of liquid–liquid and solid–supercritical fluid phase transitions in PE with molecular weight ranging from 13 600 to 120 000 in supercritical propane. In their study, it was inconclusive if the experimental data exhibited upper critical solution temperature (UCST)

or lower critical solution pressure (LCST) phase behavior due to the flatness of the pressure–composition diagrams.

Kiran et al.<sup>5</sup> reported the cloud point pressure of PE with molecular weight ranging from 2100 to 420 000 in pentane under high pressure up to 70 MPa and polymer mass fraction up to 15%. The LCST phase behavior was observed for PE in pentane at high pressure. The temperature–concentration curves were relatively flat over the mass fraction range from (0.05 to 15)%, and the cloud point pressure only increased by about 25% with molecular weight from 2100 to 420 000.

For the flash-spinning process, trichlorofluoromethane (Freon-11) had been mainly used as a solvent for PE or polypropylene since it can dissolve the polymers well under high pressures and high temperatures. However, since we have to satisfy the chlorofluorohydrocarbon regulations, manufactures of nonwoven fabrics with the flash-spinning had searched for the substitutable solvents for Freon-11. As the results of their efforts, many patents<sup>6</sup> including phase behaviors of polymer solution under high temperatures and high pressures issued by industrial companies have been reported for substitutable solvents for flash-spinning. Among them, some PE + halogenated alkane solutions have been also suggested as substitutable systems for flash-spinning.

Although we have recognized the importance of the exploration of the phase behaviors for polymer halogenated solvent systems as mentioned above, very few experimental data of the phase behaviors of polymer and halogenated solvent systems have been reported. The phase behaviors of poly(ethylene-co-methyl acrylate) in supercritical chlorodifluoromethane and propane were determined by Meilchen et al.<sup>7</sup> They also employed a different design of a variable-volume view cell<sup>7–9</sup>

\* Corresponding author. Tel.: +81-75-383-2621. Fax: +81-75-383-2623. E-mail: takenaka@alloy.polym.kyoto-u.ac.jp.

<sup>†</sup> Part of the “Gerhard M. Schneider Festschrift”.

<sup>‡</sup> Asahi Kasei Fibers Corporation.

<sup>§</sup> Kyoto University.

<sup>||</sup> Fukui University.

to observe the cloud point, respectively. LCST phase behaviors of poly(methyl methacrylate) and polycaprolactone in supercritical chlorodifluoromethane were determined by Haschets and Shine.<sup>10</sup> However, there has been no report on the phase behavior of the PE and halogenated solvent system under high pressure and high temperature.

As will be described later, it is difficult to investigate the phase behaviors of PE halogenated solvent systems because they cannot obtain a homogeneous polymer solution for PE halogenated solvent systems with the cells used in the previous experiments. To attain complete mixing of PE halogenated solvent systems, we have developed a new high-pressure cell. Then, we investigated the phase behaviors of solutions of PE with high molecular weight in hydrocarbon, halogenated hydrocarbon, and oxygen-containing hydrocarbon and their mixture at high pressure and high temperature, especially at near-supercritical and supercritical conditions of solvents. The composition dependence of the  $P, T$  cloud point curves was also determined.

## Experimental Section

**Apparatus and Operational Procedure.** The optical bomb,<sup>1</sup> the optical cell,<sup>5</sup> and the variable-volume viewing cell<sup>4,11</sup> have been used to measure cloud points under high pressure and high temperature in previous experiments. Each apparatus has a different mixing mechanism. Mixing in the optical bomb is done by rotating the cell itself. An optical cell and a variable-volume viewing cell have an external magnetic stirrer and a Teflon-coated stir bar inside the cavity of the cell. However, it is difficult to achieve homogeneity without degradation of the solutions of viscous polymer solutions since the mixing ability of both types of cells is not sufficient. In the case of polyethylene in the halogenated alkane system, especially, separated upper and lower phases with large differences of each density are difficult to remix uniformly.

To avoid the degradation of the solutions, we developed a new cell which has the following features: (1) The stirrers are directly driven by motors so that the mixture can be mixed with a powerful torque. (2) Easy control of pressure and temperature enables us to measure the cloud point quickly with high precision, thus we can avoid the effects of the degradation of samples on the determination of cloud points. (3) Since the apparatus is easily taken apart and can be cleaned completely, we can prevent any contamination resulting from degradation of the solutions. (4) Two windows are arranged on the upper side and lower side of the cell to easily distinguish whether phase separation occurs, especially in the case of separated upper and lower phases owing to the difference of specific gravity.

Figure 1 shows a schematic diagram of the vertical sectional view of the two-window high-pressure cell (Hikari-Kouatsu, Japan) used in this study. The cell made of 316 stainless steel can withstand up to 100 MPa and 573 K. The cell consists of a high-pressure vessel (128 mm o.d.  $\times$  185 mm long, working volume = 100 cm<sup>3</sup>) (A), stirrer units (B), window units (C), and a thermometer unit (D). The upper and lower windows (3) made of optically isotropic quartz have a diameter of 10 mm and a thickness of 9 mm. A Poulter-type seal<sup>12</sup> is used as the sealing method between the optical glasses and the supporting parts (2). The window units are tightened to the vessel with O-rings made of Teflon containing copper powder (4). A stirrer unit consists of a fan (6) and a scraper (5) rotating at 60 rpm. The fan makes the polymer solution to promote the forced convection inside the cell. The scraper wipes the viscous sticking polymer from the inner wall. Separated upper and lower phases owing to the difference of each specific gravity

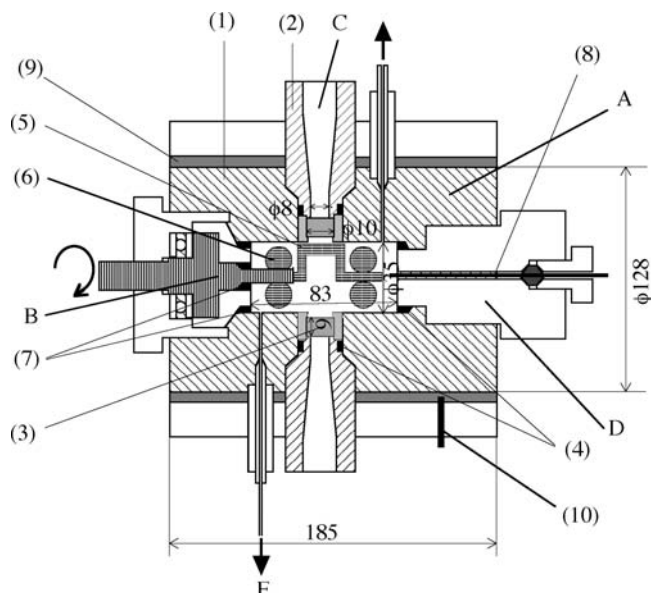


**Figure 1.** Vertical cross section of a two-window high-pressure cell. A, high-pressure vessel; B, stirrer units; C, window units; D, thermometer unit; E, pressure control system; F, exhaust; 1, cell body; 2, supporting parts; 3, optical glass; 4, O-ring; 5, scraper; 6, fan; 7, Bridgeman unsupported area seal; 8, RTD thermometer; 9, aluminum block heater; 10, PID controller.

are mixed homogeneously by the two types of stirrers. A Bridgeman unsupported area seal<sup>11</sup> (7) is used as a dynamic seal between the vessel and the shaft of a stirrer. The temperature of the vessel is controlled by an aluminum block heater (9) regulated by a PID controller (10). The fluctuation of temperature in the cell can be detected within  $\pm 0.1$  K using an RTD thermometer. A pressure transmit unit connects the pressure control and solvent delivery system to the cell. All parts can be taken apart and cleaned up easily.

Figure 2 shows a schematic diagram of the experimental arrangement. Solvent is used as a pressure transmitter to avoid contamination. Pressure is measured by an electrical pressure gauge (Nagano-Keiki, model KH15) (PG). The pressure gauge is frequently calibrated with a Heise gauge (model CC90037). RD is a safety valve. The rotary pump (PGN) is used to adjust the pressure in the cell. A high-pressure tube (shown by the dotted line) is heated to avoid the stack of polymer.

The cloud point is defined as the condition at which the mixture becomes so opaque that it is no longer possible to see the halogen light placed at the opposite window. The cloud point pressure at a given temperature is determined by the sudden increase in the turbidity with decreasing pressure, and the temperature dependence of the cloud point pressure was studied. The accuracy of  $P$  and  $T$  is  $\pm 0.01$  MPa and  $\pm 0.1$  K, respectively. They are obtained over a temperature range of (375 to 495) K.

**Materials.** The weight-averaged molecular weight  $M_w$ , polydispersity index  $M_w/M_n$ , and density of the PE used in this study are, respectively,  $1.02 \cdot 10^5$  g  $\cdot$  mol<sup>-1</sup>, 6.14, and 0.969 g  $\cdot$  cm<sup>-3</sup>. The characteristic parameters<sup>13</sup> of solvents used in this study are summarized in Table 1.  $T_c$  is the critical value of temperature. All solvents were purchased from Wako Pure Chemical Industry (extra pure grade) and Tokyo Chemical Industry (extra pure grade) and used without further purification.

## Result and Discussion

**Cloud Point Curves of PE in a Single Component Solvent.**  $P, T$  cloud point curves for PE in *n*-pentane are shown in Figure 3 for polymer volume fractions of (0.3, 0.6, 1.3, 2.0, 2.1, 3.3,

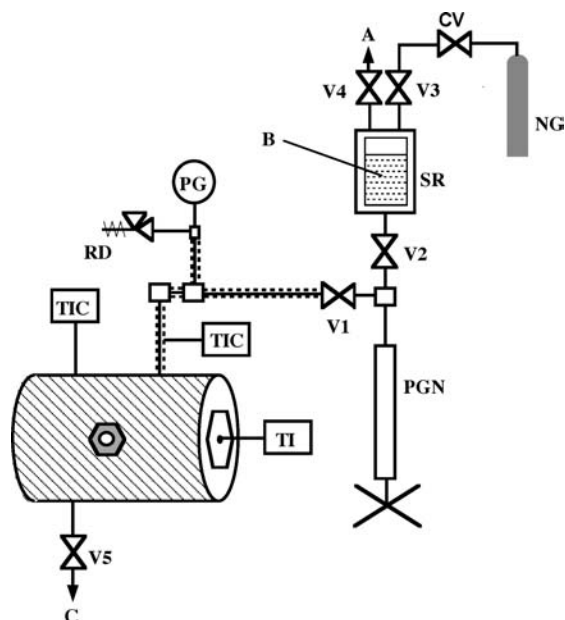


**Figure 2.** Schematic diagram of experimental arrangement. PG, electrical pressure gauge; RD, safety valve; PGN, rotary pump; TIC, PID temperature controller; V1–V5, high-pressure valves; SR, solvent tank; NG, nitrogen gas; A, solvent inlet; B, solvent; C, exhaust and vacuum.

**Table 1.** Lists of Characteristic Parameters of Solvents, Fitting Parameters (*A*, *B*, and *C*), and the Values of Cloud Point Pressure at  $T_c$  of the Corresponding Solvent,  $P_{T=T_c}$ , and the Slope of the Cloud Point Curve at  $T_c$

	$T_c$				$P_{T=T_c}$	$dP/dT_{T=T_c}$
	K	<i>A</i>	10 <i>B</i>	10 <sup>4</sup> <i>C</i>		
butane	425.20	-125.27	5.98	-5.54	28.94	0.127
2-methyl butane	460.40	-139.04	5.82	-5.10	20.80	0.112
pentane	469.70	-168.88	6.94	-6.27	18.74	0.116
2,2-dimethylbutane	488.80	-130.03	5.11	-4.31	16.52	0.089
2-methyl pentane	497.50	-177.08	6.94	-6.19	15.00	0.078
2,3-dimethylbutane	500.00	-193.04	7.48	-6.66	14.61	0.083
hexane	507.50	-125.74	4.53	-3.50	14.06	0.098
3-methylpentane	504.50	-128.51	4.67	-3.66	13.92	0.098
heptane	540.30	-311.25	11.8	-10.9	9.01	0.001
chloroethane	460.40	-45.84	1.41	0	19.18	0.141
2-chloropropane	485.00	-21.94	1.61	0	18.89	0.161
trichlorofluoromethane	471.20	-59.86	1.71	-0.267	14.77	0.146
dichloromethane	510.00	-91.77	2.08	0	14.45	0.208
2-chlorobutane	520.60	-390.30	14.1	-12.3	12.65	0.131

8.4, and 18.1) %. The region above a cloud point curve is a one-phase region. The two-phase region is attained either by an increase in temperature at constant pressure or by a decrease in pressure at constant temperature so that the solutions have UCSP and LCST phase diagrams. The cloud point pressures for the various volume fractions had similar slopes. Each cloud point curve was well fitted with  $P/\text{MPa} = A + B(T/\text{K}) + C(T/\text{K})^2$ . The  $P, T$  cloud point curves for PE in pentane are compared with a similar system reported by Kiran and Zhuang. Their sample had a narrow molecular weight with  $M_w = 1.08 \cdot 10^5$  and  $M_w/M_n = 1.32$ , which has a  $M_w$  almost equal to and a  $M_w/M_n$  different from our sample. Their experimental temperature range was from (420 to 470) K, while our experimental data range is from (440 to 510) K. By comparison at  $440 \text{ K} < T < 470 \text{ K}$ , our cloud point curves locate at higher pressure than their results, although the slopes of both curves are similar. This difference may be due to the effect of molecular weight distribution.

$P, T$  cloud point curves for PE in trichlorofluoromethane and hexane are shown for different polymer solutions at various

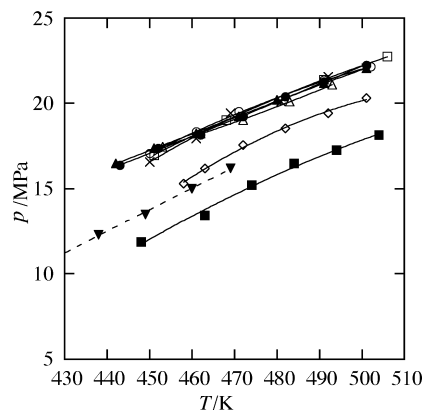


**Figure 3.**  $P, T$  cloud point curves for polyethylene in pentane for polymer volume fractions of (0.3, 0.6, 1.3, 2.0, 2.1, 3.3, 8.4, and 18.1) %. The dashed line represents Kiran's data for polyethylene ( $M_w = 108\,000$ ) in pentane with a weight fraction of 3.0%.  $\times$ , 0.3%;  $\circ$ , 0.6%;  $\square$ , 1.3%;  $\bullet$ , 2.0%;  $\triangle$ , 2.1%;  $\blacktriangle$ , 3.3%;  $\diamond$ , 8.4%;  $\blacksquare$ , 18.1%;  $\blacktriangledown$ , Kiran's data.

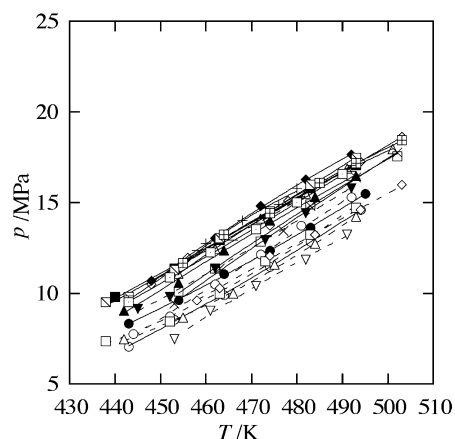


**Figure 4.**  $P, T$  cloud point curves for polyethylene in trichlorofluoromethane for polymer volume fractions of  $\times$ , 0.12%;  $-\circ-$ , 0.20%;  $-\square-$ , 0.25%;  $-\bullet-$ , 0.40%;  $-\triangle-$ , 0.49%;  $-\blacktriangle-$ , 0.80%;  $-\blacklozenge-$ , 1.53%;  $-\blacksquare-$ , 1.60%;  $-\diamond-$ , 2.07%;  $-\blacklozenge-$ , 2.42%;  $-\square-$ , 2.64%;  $-\blacksquare-$ , 3.06%;  $-\square-$ , 5.01%;  $-\blacklozenge-$ , 7.50%;  $\blacktriangledown$ , 10.03%;  $-\circ-$ , 12.54%;  $-\square-$ , 15.04%;  $-\diamond-$ , 18.06%;  $-\blacklozenge-$ , 19.43%; and  $-\blacktriangledown-$ , 20.05%.

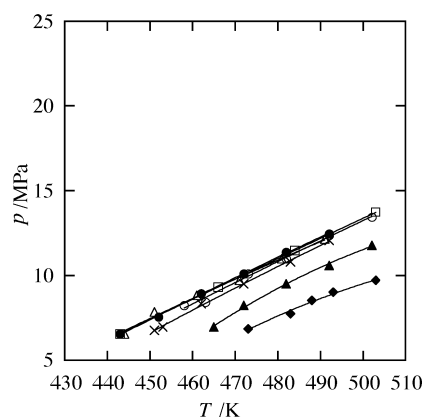


**Figure 5.**  $P, T$  cloud point curves for polyethylene in hexane for a polymer volume fraction of (0.34, 0.67, 1.35, 2.06, 3.43, 8.82, and 18.06) %.  $\times$ , 0.34%;  $\circ$ , 0.67%;  $\square$ , 1.35%;  $\bullet$ , 2.06%;  $\triangle$ , 3.43%;  $\blacktriangle$ , 8.82%;  $\blacklozenge$ , 18.06%.

concentrations in Figures 4 and 5, respectively. The region above a cloud point curve is a one-phase region. Each cloud point curve was also well fitted with  $P/\text{MPa} = A + B(T/\text{K}) + C(T/\text{K})^2$ .

Figure 6 shows the pressure as a function of volume fraction ( $P, \phi$ ) phase diagram for PE in pentane, hexane, and trichloro-

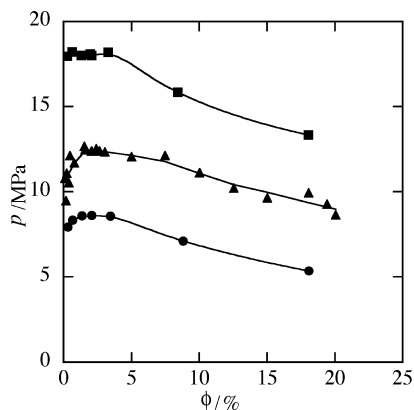


**Figure 6.**  $P, \phi$  cloud point curves of polyethylene in pentane, trichlorofluoromethane, and hexane at 473 K. ■, pentane; ▲, trichlorofluoromethane; ●, hexane.

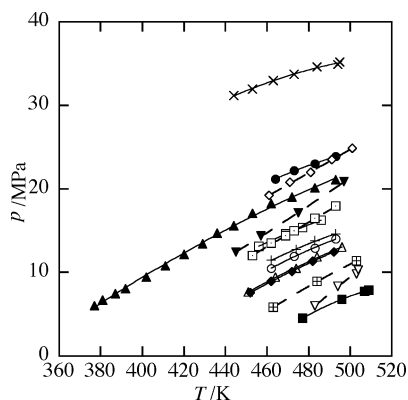
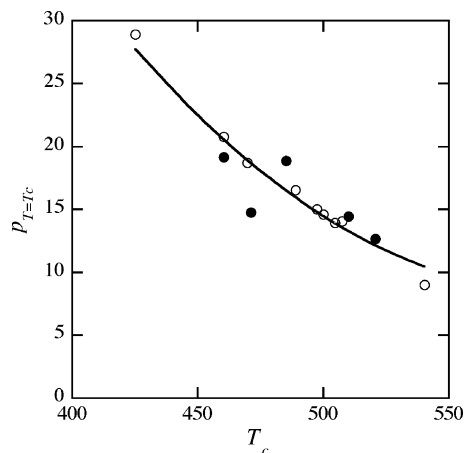


**Figure 7.**  $P, T$  cloud point curves of polyethylene with different solvents at a polymer volume fraction of 2%. Hydrocarbons are butane, 2-methylbutane, pentane, 2,2-dimethylbutane, 2-methylpentane, 2,3-dimethylbutane, hexane, 3-methylpentane and heptane. Halogenated hydrocarbons are chloroethane, 2-chloropropane, trichlorofluoromethane, 2-chlorobutane and dichloromethane. ×, Butane; ●, 2-Methylbutane; ▲, Pentane; □, 2,2-Dimethylbutane; +, 2-Methylpentane; ○, 2,3-dimethylbutane; ◆, Hexane; △, 3-Methylpentane; ■, Heptane; ◇, Chloroethane; ▼, 2-Chloropropane; ⊠, Trichlorofluoromethane; ⊞, 2-Chlorobutane; ▽, Dichloromethane. Solid lines are hydrocarbons and dashed lines are halogenated hydrocarbons.

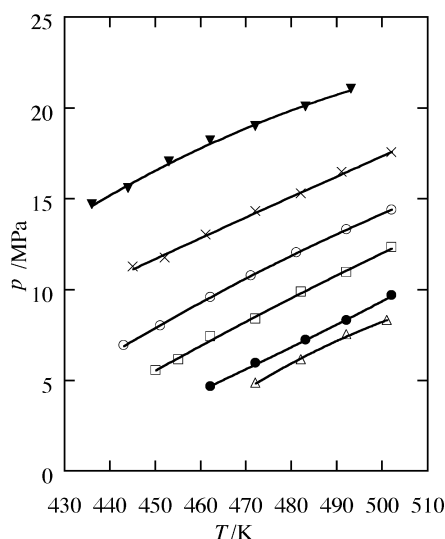
fluoromethane at 473 K. The cloud point pressure was estimated from the fitting results of the cloud point curves with  $P/\text{MPa} = A + B(T/K) + C(T/K)^2$  in the  $P, T$  parameter space. The figure shows that it was relatively flat over the composition range studied. The regions above each curve correspond to the single-phase regions. The curves represent UCSP. The figure indicates that the critical polymer volume fractions are about 2%, which is independent of the type of solvent.

Figure 7 shows the  $P, T$  cloud point curves for polyethylene in different hydrocarbons and halogenated hydrocarbon at a polymer volume fraction of 2%. Hydrocarbons are butane, 2-methylbutane, pentane, 2,2-dimethylbutane, 2-methylpentane, 2,3-dimethylbutane, hexane, 3-methylpentane, and heptane. Halogenated hydrocarbons are chloroethane, 2-chloropropane, trichlorofluoromethane, 2-chlorobutane, and dichloromethane. Each cloud point curve was well fitted with  $P/\text{MPa} = A + B(T/K) + C(T/K)^2$ . The solid lines are hydrocarbon, and the dashed lines are halogenated hydrocarbon. The region above each cloud point curve is the one-phase region.  $A$ ,  $B$ , and  $C$  values are listed in Table 2.

Then the values of cloud point pressure at  $T_c$  of the corresponding solvent,  $(P)_{T=T_c}$ , and the slope of the cloud point curve at  $T_c$ ,  $(dP/dT)_{T=T_c}$ , were determined. In the case of heptane



**Figure 8.** Plot of  $P_{T=T_c}$  at  $T_c$  for polyethylene in hydrocarbons (open mark) and halogenated hydrocarbons (closed mark) as a function of  $T_c$  of each solvent. ○,  $P_{T=T_c}$  vs  $T_c$  of hydrocarbons; ●,  $P_{T=T_c}$  vs  $T_c$  of halogenated hydrocarbons.



**Figure 9.**  $P, T$  cloud point curves for polyethylene in mixed solvents. These are mixed with different hydrocarbon and pentane at the volume ratio of 50/50. Hydrocarbons are hexane, heptane, octane, cyclohexane, and decane. The  $P, T$  cloud point curve for polyethylene in pentane is also show in this figure. ×, Hexane + Pentane; ○, Heptane + Pentane; □, Octane + Pentane; ●, Cyclohexane + Pentane; △, Decane + Pentane; ▼, Pentane.

and dichloromethane,  $(P)_{T=T_c}$  and  $(dP/dT)_{T=T_c}$  are determined from the extrapolation of the fitted equations. The calculated results are shown in Table 1. For all systems,  $(dP/dT)_{T=T_c}$  are positive in these experimental conditions.

Figure 8 shows  $(P)_{T=T_c}$  for PE in hydrocarbon (open mark) and polyethylene in halogenated hydrocarbon (closed mark) plotted against critical temperature,  $T_c$ , of each solvent. The good correlation between  $(P)_{T=T_c}$  and  $T_c$  is found for PE in hydrocarbon and the halogenated hydrocarbon system. Since  $T_c$  is correlated to the free volume of solvent, the good correlation indicates that the free volume change in mixing is dominant in the solubility of the PE solutions.

**Cloud Point Curves of PE in Binary Solvents.** We investigated the effects of mixing of solvents on phase diagrams. First we examined the binary solvents consisting of different hydrocarbon and pentane at the volume ratio of 50/50. Figure 9 shows the  $P, T$  cloud point curves for PE in hydrocarbon + pentane at a polymer volume fraction of 2%. The solubility increases with molecular weight of hydrocarbon except for cyclohexane. Cyclohexane increases the solubility more than

**Table 2.** List of Fitting Parameters (*A*, *B*, and *C*) of Binary Solvents

	<i>A</i>	10 <i>B</i>	10 <sup>4</sup> <i>C</i>
hexane + pentane	-51.22	1.64	-0.54
heptane + pentane	-127.02	4.57	-3.49
octane + pentane	-92.95	3.00	-1.79
cyclohexane + pentane	-11.36	-0.05	1.77
decane + pentane	-282.23	1.07	-9.74
trichlorofluoromethane + pentane	-64.20	2.24	-1.10
dibromodifluoromethane + pentane	-48.85	1.38	0
bromomethane + pentane	-37.03	0.82	-0.46
dichloromethane + pentane	-68.34	1.81	-0.28
trichloromethane + pentane	-81.39	2.66	-0.81
HCFC123 + pentane	-35.34	2.06	-1.55
1,2-dichloro-1,2-difluoroethane + pentane	45.28	-1.96	3.11
chloroethane + pentane	109.39	-5.16	6.91
1-bromo-1-chloro-2,2,2-trifluoroethane + pentane	-119.59	4.55	-3.50
1,1-dichloroethane + pentane	-40.56	0.66	0.86
1,2-dichloroethane + pentane	45.595	-2.89	4.49
1,1,2,2-tetrachloro-1,2-difluoroethane + pentane	-192.93	7.19	-6.22
<i>cis</i> -1,2-dichloroethylene + pentane	38.42	-2.70	4.32
iodoethane + pentane	-45.83	1.08	0
1,2-dichloroethane + pentane	-58.09	1.33	0
trichloroethylene + pentane	-61.73	1.38	0
1,1,2-trichloroethane + pentane	-56.845	1.24	0
1-chloropropane + pentane	-105.01	3.49	-2.11
2-bromopropane + pentane	64.82	-3.61	5.21
1-bromopropane + pentane	-27.06	0.03	1.48
1,2-dichloropropane + pentane	-93.91	2.79	-1.49
acetone + pentane	969.86	-37.19	36.83
isopropanol + pentane	490.49	-19.12	19.64
1-propanol + pentane	482.68	-19.57	20.56
methyl ethyl ketone + pentane	-79.88	3.15	-2.37
<i>n</i> -butanol + pentane	172.35	-7.75	9.13
diethyl ketone + pentane	12.16	-1.23	2.49
dibutyl + pentane	-62.99	1.82	-0.70
tetrahydropyran + pentane	13.22	-1.64	3.09
tetrahydrofuran + pentane	-174.15	6.04	-4.77
1,4-dioxane + pentane	-351.21	13.30	-12.26

hexane. This result suggests that the addition of bulky molecules enhances the solubility of PE. Each cloud point curve was well fitted with  $P/\text{MPa} = A + B(T/K) + C(T/K)^2$ . *A*, *B*, and *C* values are listed in Table 2.

The binary solvents consisting of different halogenated hydrocarbon and pentane at the volume ratio of 50/50 are examined. The *P*, *T* cloud point curves for PE in halogenated hydrocarbon + pentane are shown in Figures 10 to 12. The polymer volume fraction was 2%. As shown in Figures 10 to 12, the increase in the number of halogens in a halogenated

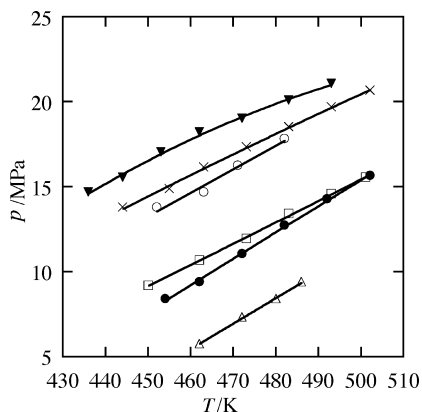


**Figure 10.** *P*, *T* cloud point curves for polyethylene in mixed solvents. These are mixed with different hydrocarbon and pentane at the volume ratio of 50/50. Halogenated hydrocarbons are trichlorofluoromethane, dibromodifluoromethane, bromomethane, dichloromethane, and trichloromethane. The *P*, *T* cloud point curve for polyethylene in pentane is also shown in this figure. x, Trichlorofluoromethane + Pentane; o, Dibromodifluoromethane + Pentane; □, Bromomethane + Pentane; ●, Dichloromethane + Pentane; △, Trichloromethane + Pentane; ▼, Pentane.

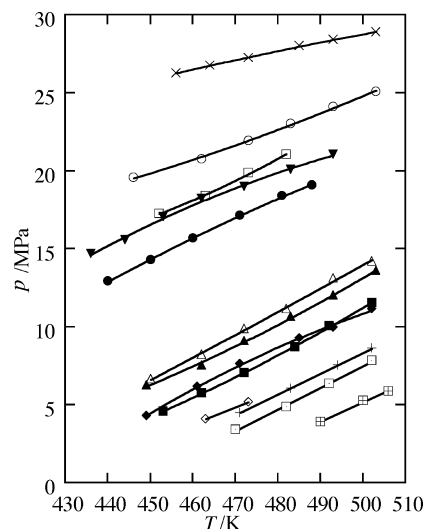


**Figure 11.** *P*, *T* cloud point curves for polyethylene in binary solvents. These are mixed with different halogenated hydrocarbon and pentane at the volume ratio of 50/50. Halogenated hydrocarbons are HCFC123, 1,2-dichloro-1,2-difluoroethane, chloroethane, 1-bromo-1-chloro-2,2,2-trifluoroethane, 1,1-dichloroethane, 1,2-dichloroethylene, 1,1,2,2-tetrachloro-1,2-difluoroethane, *cis*-1,2-dichloroethylene, iodoethane, 1,2-dichloroethane, trichloroethylene, and 1,1,2-trichloroethane. The *P*, *T* cloud point curve for polyethylene in pentane is also shown in this figure. x, HCFC123 + Pentane; o, 1,2-Dichloro-1,2-difluoroethane + Pentane; □, Chloroethane + Pentane; ●, 1-Bromo-1-chloro-2,2,2-trifluoroethane + Pentane; △, 1,1-Dichloroethane + Pentane; ▲, 1,2-Dichloroethylene + Pentane; ◆, 1,1,2,2-Tetrachloro-1,2-difluoroethane + Pentane; ■, *cis*-1,2-Dichloroethylene + Pentane; ◇, Iodoethane + Pentane; +, 1,2-Dichloroethane + Pentane; □, Trichloroethylene + Pentane; ⊞, 1,1,2-Trichloroethane + Pentane; ▼, Pentane.

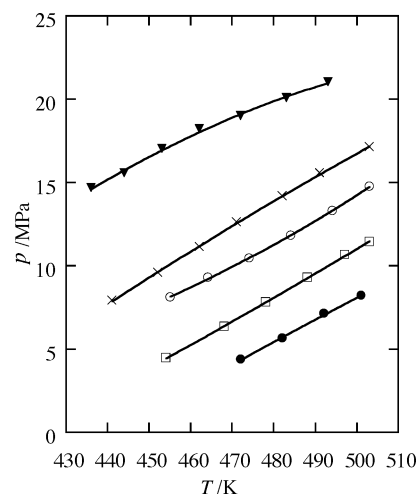


**Figure 12.** *P*, *T* cloud point curves for polyethylene in mixed solvents. These are mixed with different halogenated hydrocarbon and pentane at the volume ratio of 50/50. Halogenated hydrocarbons are 1-chloropropane, 2-bromopropane, 1-bromopropane and 1,2-dichloropropane. The *P*, *T* cloud point curve for polyethylene in pentane is also shown in this figure. x, 1-Chloropropane + Pentane; o, 2-Bromopropane + Pentane; □, 1-Bromopropane + Pentane; ●, 1,2-Dichloropropane + Pentane; ▼, Pentane.

hydrocarbon molecule enhances the solubility of polymer. All cloud point curves have similar slopes irrespective of the kind of halogenated hydrocarbon. *A*, *B*, and *C* values estimated from fitting procedures with  $P/\text{MPa} = A + B(T/K) + C(T/K)^2$  are listed in Table 2.

Figure 13 shows the *P*, *T* cloud point curves for polyethylene in binary solvents of oxygen-containing hydrocarbon/pentane = 50/50 (vol/vol) at the polymer volume fraction 2%. Contrary

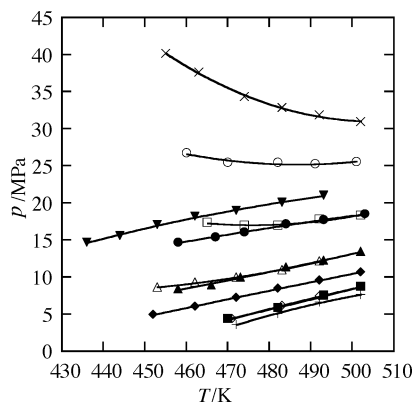


**Figure 13.**  $P, T$  cloud point curves for polyethylene in mixed solvents. These are mixed with different oxygen-containing hydrocarbon and pentane at the volume ratio of 50/50. Solvents are acetone, isopropanol, 1-propanol, methyl ethyl ketone, *n*-butanol, diethyl ketone, dibutyl ether, tetrahydropyran, tetrahydrofuran, and 1,4-dioxane. The  $P, T$  cloud point curve for polyethylene in pentane is also shown in this figure.  $\times$ , Acetone + Pentane;  $\circ$ , Isopropanol + Pentane;  $\square$ , 1-Propanol + Pentane;  $\bullet$ , Methyl ethyl ketone + Pentane;  $\triangle$ , *n*-Butanol + Pentane;  $\blacktriangle$ , Diethyl ketone + Pentane;  $\blacklozenge$ , Dibutyl ether + Pentane;  $\blacksquare$ , Tetrahydropyran + Pentane;  $\diamond$ , Tetrahydrofuran + Pentane;  $+$ , 1,4-Dioxane + Pentane;  $\nabla$ , Pentane.

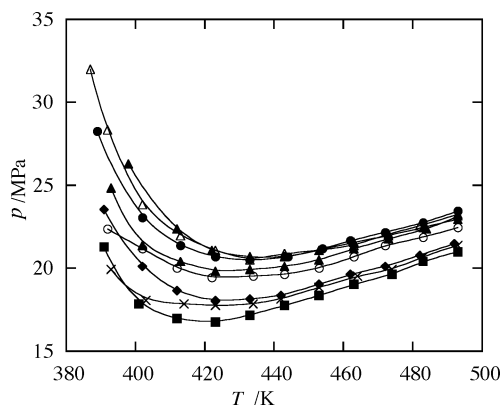


**Figure 14.**  $P, T$  cloud point curves for polyethylene in mixed solvent of HCFC123 and cyclohexane at the volume ratio of 75/25 for polymer volume fractions of (0.1, 0.26, 0.52, 1.04, 2.08, 4.16, 8.33, and 18.1) %.  $\times$ , 0.1 %;  $\circ$ , 0.26 %;  $\triangle$ , 0.52 %;  $\bullet$ , 1.04 %;  $\square$ , 2.08 %;  $\blacktriangle$ , 4.16 %;  $\blacklozenge$ , 8.33 %;  $\blacksquare$ , 12.5 %.

to the cloud point curves in hydrocarbon + pentane and halogenated hydrocarbon + pentane, the slope of the  $P, T$  cloud point curves of acetone, isopropanol, and 1-propanol becomes negative or almost zero. The change in the slope may be induced by the existence of oxygen. On the other hand, the tendency of cloud point curves of the other solutions is similar to those of hydrocarbon + pentane and halogenated hydrocarbon + pentane. This is because the effects of the longer hydrocarbon part become dominant on the solubility of the solutions.  $A$ ,  $B$ , and  $C$  values obtained by fitting with  $P/\text{MPa} = A + B(T/\text{K}) + C(T/\text{K})^2$  are listed in Table 2.

**Phase Diagram of PE in HCFC123 + Cyclohexane.** Recently, HCFC123 has been used widely as a solvent for PE instead of trichlorofluoromethane (Freon-11). It is important to explore the effects of mixing hydrocarbon with HCFC123 on the phase diagram.

$P, T$  cloud point curves for PE in the binary solvent of HCFC123 and cyclohexane at the volume ratio of 75/25 are shown in Figure 14 for different polymer concentrations. The  $P, T$  cloud point curves exhibit a minimum around  $T = 420$  K, indicating that the  $T, \phi$  phase diagram at a certain pressure exhibits both LCST and UCST.

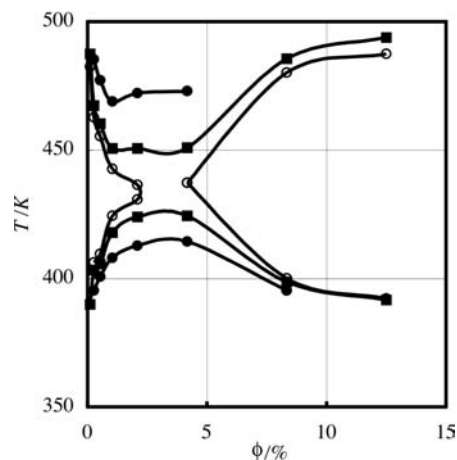


**Figure 15.**  $T, \phi$  cloud point curves of polyethylene in mixed solvent of HCFC123 and cyclohexane at the volume ratio of 75/25 at  $\bullet$ , 22.00 MPa;  $\blacksquare$ , 21.00 MPa;  $\circ$ , 20.66 MPa.

Figure 15 shows the temperature–composition  $T, \phi$  phase diagram for PE in binary solvent of HCFC123 and cyclohexane at the volume ratio of 75/25 at different pressure. The  $T, \phi$  phase diagram changes from an hourglass shape to a LCST + UCST type with pressure.

## Conclusions

The  $P, T$  cloud point curves at volume fraction of 2 % high molecular weight polyethylene in hydrocarbon, halogenated hydrocarbon, oxygen-containing hydrocarbon, and their mixture at high temperature and high pressure were measured by using a newly designed high-pressure optical cell. It was found that the cloud point pressure of the solution has a good correlation with the critical temperature ( $T_c$ ) of solvents.

We investigated the phase diagrams of PE in binary solvents. In the case of hydrocarbon + pentane, the increase in molecular weight of hydrocarbon molecules enhances the solubility of the solutions. The solubility of PE in halogenated hydrocarbon + pentane increases with the number of halogens in halogenated hydrocarbon.

Finally,  $P, T$  cloud point curves for PE in the binary solvent of HCFC123/cyclohexane with a volume ratio of 75/25 (vol/vol) were measured as a function of  $\phi$ . The  $P, T$  cloud point curves at observed  $\phi$  exhibit a minimum around  $T = 420$  K, and the  $T, \phi$  phase diagram changes from an hourglass shape to LCST + UCST-type with pressure.

## Literature Cited

- (1) Ehrlich, P.; Kurpen, J. J. Phase equilibria of polymer–solvent systems at high pressures near their critical loci: polyethylene with *n*-alkanes. *J. Polym. Sci., Part A* **1963**, *1*, 3217–3229.
- (2) De Loos, T. W.; Poot, W.; Diepen, G. A. M. Fluid phase equilibria in the system polyethylene + ethylene. 1. Systems of linear polyethylene + ethylene at high pressure. *Macromolecules* **1983**, *16*, 111–117.
- (3) De Loos, T. W.; Lichtenthaler, R. N.; Diepen, G. A. M. Fluid phase equilibria in the system polyethylene + ethylene. 2. Calculation of cloud curves for systems of linear polyethylene + ethylene. *Macromolecules* **1983**, *16*, 117–121.
- (4) Condo, P. D., Jr.; Colman, E. J.; Ehrlich, P. Phase equilibria of linear polyethylene with supercritical propane. *Macromolecules* **1992**, *25*, 750–753.
- (5) Kiran, E.; Zhuang, W. Solubility of polyethylene in *n*-pentane at high pressures. *Polymer* **1992**, *33*, 5259–5263.
- (6) USP 5,032,326; USP 5,081,177; USP 5,023,025; EP 0357381 A2; EP 0361684 A1; EP 0407953 A2; EP 0357364 A4; EP 0414498 A2; Jpn Kokai Tokkyo Koho H2-139408; Jpn Kokai Tokkyo Koho H2-160909; Jpn Kokai Tokkyo Koho H3-76809; Jpn Kokai Tokkyo Koho H3-

- 152209, Jpn Kokai Tokkyo Koho H5-263308, Jpn Kokai Tokkyo Koho H5-279273, Jpn Kokai Tokkyo Koho H5-295612, Jpn Kokai Tokkyo Koho H5-295613, Jpn Kokai Tokkyo Koho H6-41810, Jpn Kokai Tokkyo Koho H6-41811, Jpn Kokai Tokkyo Koho H6-116808, Jpn Kokai Tokkyo Koho H6-116809.
- (7) Meilchen, M. A.; Hasch, B. M.; McHugh, M. A. Effect of copolymer composition on the phase behavior of mixtures of poly(ethylene-co-methyl acrylate) with propane and chlorodifluoromethane. *Macromolecules* **1991**, *24*, 4874–4882.
- (8) Seckner, A. J.; McClellan, A. K.; McHugh, M. A. High-pressure solution behavior of the polystyrene–toluene–ethane system. *AIChE. J.* **1988**, *34*, 9.
- (9) McHugh, M. A.; Guckes, T. L. Separating polymer solutions with supercritical fluids. *Macromolecules* **1985**, *18*, 674.
- (10) Haschets, C. W.; Shine, A. D. Phase behavior of polymer-supercritical chlorodifluoromethane solutions. *Macromolecules* **1993**, *26*, 5052–5060.
- (11) Saraf, V. P.; Kiran, E. Supercritical fluid–polymer interactions: phase equilibrium data for solutions of polystyrenes in *n*-butane and *n*-pentane. *Polymer* **1988**, *29*, 2061–2065.
- (12) Sherman, W. F.; Standmuller, A. A. *Experimental Techniques in High-Pressure Research*; Wiley: New York, 1987.
- (13) Reid, R. C.; Prausnitz, J. M.; Poling, B. E. *The Properties of GASES & LIQUIDS*; McGRAW-HILL: 1988.

Received for review November 28, 2008. Accepted March 31, 2009.

JE800918Q